Aerosol radiative forcing estimated from ground-based sky radiation measurements over East Asia

Kim, Dohyeong[1], B. J. Sohn[1], T. Nakajima[2], I. Okada[3], T. Takamura[3]
School of Earth and Environmental Sciences, Seoul National University[1],
Center for Climate System Research, University of Tokyo[2],
Center for Environmental Remote Sensing, Chiba University[3]

Abstract

The clear sky radiative forcings of aerosols were evaluated over East Asia. We first investigated optical characteristics of aerosol using sky radiation measurements. An algorithm of Nakajima et al. (1996) is used for retrieving aerosol parameters such as optical thickness, Ångström exponent, single scattering albedo, and size distribution from sky-radiation measurements, which then can be used for examining spatial and temporal variations of aerosol. Obtaining aerosol radiative forcing at TOA and surface, a radiative transfer model is used with inputs of obtained aerosol parameters and GMS-5 satellite-based cloud optical properties. Results show that there is a good agreement of simulated downwelling radiative flux at the surface with observation within 10 W m^{-2} rms errors under the clear sky condition. However, a relatively large difference up to 40 W m^{-2} rms error is found under the cloudy sky condition. The computed aerosol radiative forcing at the surface shows downward flux changes ranging from -100 to -170 W m^{-2} per unit aerosol optical thickness at 0.7 μm. The different values of aerosol radiative forcing among the stations is mainly due to the differences in single scattering albedo ($\omega_{0.7}$) and asymmetric parameter (g_1) related to the geographical and seasonal variations.

1. Introduction

It has been well known that aerosols can give profound impact on global and regional climates, both by directly interfering solar radiation and by indirectly modifying cloud microphysics (e.g., Kaufman et al., 1997; Russell et al., 1999; Satheesh et al., 1999; Lohmann et al., 2000; Nakajima et al., 2001). Global average of the associated annual radiative forcing by aerosols ranges from 0 to –2 W m^{-2} that is comparable to the forcing induced by greenhouse gas increases during the last century (e.g., Charlson et al., 1992; Shine and Forster, 1999; Hansen et al., 2000; IPCC, 2001). However, it is noted that those values are subject to a high degree of uncertainty by more than a factor of two (Schwartz, 1996; Haywood and Ramaswamy, 1998; Jacobson, 2001). Accordingly, IPCC (2001) reported that uncertainties by different contributing factors should be resolved in order to estimate the overall uncertainty in the direct/indirect forcing estimates.

Because of importance of aerosols in the climate change studies, field experiments are much needed to reduce those uncertainties. Several field experiments such as Aerosol Characterization Experiment [ACE1 and ACE2], Tropospheric Aerosol Radiative Forcing Observational Experiment [TARFOX] (Russell et al., 1999) and Indian Ocean Experiment [INDOEX] (Ramanathan et al., 1996) were taken places to observe the optical and chemical properties of aerosols, which can be used for parameterizations for climate model. In line with those field experiments, Aerosol Robotic Network [AERONET] also collects the aerosol optical properties based on the world-wide ground-based aerosol monitoring network consisting of automatic sun-sky scanning spectral radiometers.

On the other hand, as a part of the GAME/AAN (GEWEX Asian Monsoon Experiment/ Asian AWS Network) a ground-based aerosol/radiation observation network named as the SKYNET was established. In order to study the role of aerosol in climate over the Asian continent, sky radiance data as well as solar radiative fluxes are measured at the SKYNET observation sites. The primary objective of the SKYNET is to estimate direct and indirect radiative forcings of aerosols on climatological time and space scales. In determining the forcing over the Asian continent, we calculate downward radiative fluxes at the surface using a radiative transfer model in which optical properties derived from SKYNET observations are used as inputs. Radiation fluxes at the top of the atmosphere (TOA) are also calculated by matching the calculated surface radiation flux to measured values.

2. Surface measurements of solar radiation

The solar radiation data of Sri-Samrong (17.17°N, 99.87°E) in Thailand and Mandalgovi (45.59°N, 106.19°E) in Mongolia, Dunhuang (40.16°N, 94.80°E), Yinchuan (38.48°N, 106.22°E) in China measured from 1998 to 2000, are analyzed in order to characterize the regional background aerosol optical properties and their effect on the surface radiation budget. Also analyzed are data collected from surface solar radiation sites at Anmyon-Do (36.52°N, 126.32°E) during the springtime of 1998 to 2000, and Kosan (33.29N, 126.17E) during April of 2001 in Korea, and Amami-Oshima (28.44°N, 129.70°E) during April of 2001 in Japan where the measured solar radiations reflect more of aerosol characteristics in coastal and marine environments, and thus we can examine the aerosol influences on surface solar radiation under such environments.

2.1 Sky radiometer data

Measurements of direct and diffuse solar radiation are taken with the sky radiometer (PREDE, POM-01L) at the wavelength of 315, 400, 500, 675, 870, 940, and 1020 nm. The aerosol optical thickness, size distribution, single-scattering albedo, and complex refractive index were derived by using the SKYRAD.pack retrieval software, which consists of a radiative transfer code as well as linear and nonlinear inversion scheme (Nakajima et al., 1996b). The aerosol optical thickness, $\tau_a(\lambda)$, is defined as:

$$\tau_a(\lambda) = \int_{rm}^{rM} \pi r^2 Q_{ext}(x,m) n(r) dr \qquad (1)$$

where Q_{ext} is the efficiency factor for extinction as given by Mie theory for spherical particles, $x=(2\pi/\lambda)r$ is size parameter, $n(r)$ is columnar radius distribution of aerosol, r_m and r_M are minimum and maximum aerosol radii, respectively, and $m=m_r - im_i$ is aerosol complex refractive index.

2.2 Solar radiative flux data

Pyranometer is used for measuring total downward solar fluxes and diffused solar radiative fluxes by solar occultation method in the wavelength region between 0.3 and 2.8 μm to avoid the emission for longer wavelength. Direct solar fluxes are estimated by the pyrheliometer, which measures the intensity of a radiant beam at normal incidence coming only from the solar disk in about 5 degree of circumsolar radiation.

3. Results

3.1 Analyses of the sky radiometer data

In order to examine the optical characteristics as a wavelength dependence of optical thickness we present the Ångström exponent α

$$\tau_{a\lambda} = \tau_{0.5}\left(\frac{\lambda}{0.5}\right)^{-\alpha} \qquad (2)$$

where λ's are wavelengths. We show the scatterplot of daily averaged $\tau_{0.5}$ versus α in Fig. 1. Mandalgovi shows a large α variation from near zero to 2.0 while significant portion of AOTs are located between 0 and 0.5. On the other hand, Dunhuang, which is located in the east of Taklimakan desert, shows a much smaller range of α while wider variation of AOT from 0 to 1.8. Patterns found in Yinchuan show a type of bundle centered around 0.5. However, all three sites show a general negative correlation between $\tau_{0.5}$ and α when α is smaller than 0.5. Smaller values of α and negatively correlated patterns are generally well-known characteristics for dust particles (Nakajima et al. 1989; Kaufman et al. 1994). In winter and spring, we find large α (1.0-2.0) and $\tau_{0.5}$ that can be explained by an influence of biomass burning at Sri-Samrong. When $\tau_{0.5}$ is higher than 0.5, α is a leveling off with some populations of values ranging from 1.3 to 1.9, which are similar to patterns and values measured for biomass burning aerosols in Amazonia (Eck et al., 1999), in Zambia (Eck et al., 2001), and for smoke from boreal forest fires (Markham et al., 1997). In Anmyon, located at the Korean coastal region, various sizes of aerosol particles are found as seen in α ranging from 0.2 to 1.5. We can clearly see the features of Asian dust with small α (< 0.5) and large $\tau_{0.5}$ at Anmyon (April of 1998 and 2000), Kosan (April of 2001) and Amami-Oshima (April of 2001).

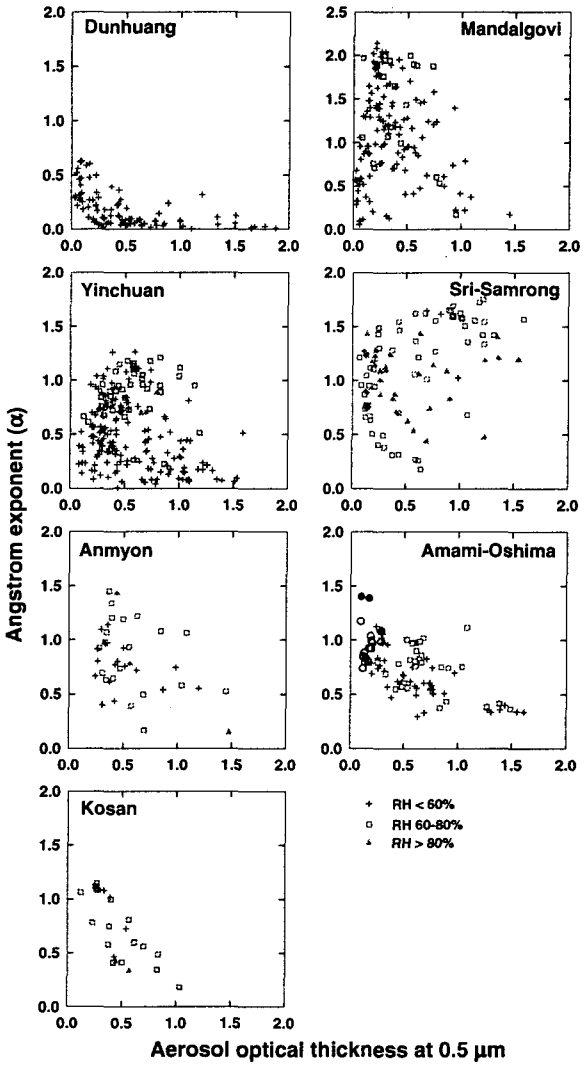

Fig. 1: Scatterplots of the Ångström exponent versus aerosol optical thickness at the wavelength of 0.5 μm.

3.2 Simulation of surface solar radiative flux

Surface solar radiative fluxes are integrated over wavelengths from 0.3 to 2.8 μm using the radiative transfer model (rstar5b) developed by Nakajima et al. (1988). For the calculation we used the measured aerosol optical properties derived from sky radiation measurements. Retrieved aerosol optical properties, such as aerosol optical thickness, size distribution, are used for describing the atmospheric aerosol under clear sky condition. For the simulation under cloudy sky condition, we used cloud fraction and cloud optical thickness, which are retrieved from GMS-5 measurements (Okada et al., 2000). Random cloud overlapping is applied for the vertical distribution of clouds. For the atmospheric

profiles, we used 6-hourly NCEP (National Centers for Environmental Prediction) reanalysis data and total ozone amounts from TOMS (Total Ozone Mapping Spectrometer) are used for calculating ozone absorption.

Fig. 2(a) shows simulation results under clear sky condition, which was determined by examining time series of surface measured solar radiative fluxes for a given local time in interest. The comparison between estimated and measured fluxes at Mandalgovi in 1998 shows a good agreement within 10 W m^{-2}. The diffuse fluxes at Sri-Samrong in March show overestimation of the simulated solar fluxes than surface measured fluxes, but in December 1998, the simulated solar fluxes show underestimates. The discrepancy is likely due to inaccurate input parameters such as water vapor amount, aerosol absorption index (absolute value of imaginary part of the aerosol refractive index), and aerosol vertical structure under clear sky condition. Furthermore, surface fluxes much depend on the loadings of atmospheric gases and aerosols even at one fixed station. Considering the fact that atmospheric conditions in the high-latitude dry area are less variant in comparison with low-latitude moist Sri-Samrong area, the more agreement found in Madalgovi manifests the impact of input parameters on uncertainties in derived surface radiation budget. More accurate retrievals of aerosol optical characteristics should reduce the differences between simulated and measured solar fluxes.

Fig. 2(b) shows simulation results under the cloudy sky condition, which was determined by using GMS-5 cloud fraction and cloud optical thickness. For sky radiometer is not available in cloudy sky condition, we should use the aerosol optical properties via time interpolation. The results at Mandalgovi show overestimates in lower flux sides. By contrast, simulated results in Sri-Samrong show overestimates if measured values are located between 100 and 200 W m^{-2}, which represents underestimation of cloud optical thickness from GMS-5 image data.

The rms (root mean square) errors of Mandalgovi and Sri-Samrong are 6.3 and 9.7 W m^{-2} under the clear sky condition, 36.6 and 42.9 W m^{-2} under the cloudy sky condition, respectively. For simulation of surface solar radiation under the cloudy sky condition, more accurate retrieval of cloud optical thickness should be needed.

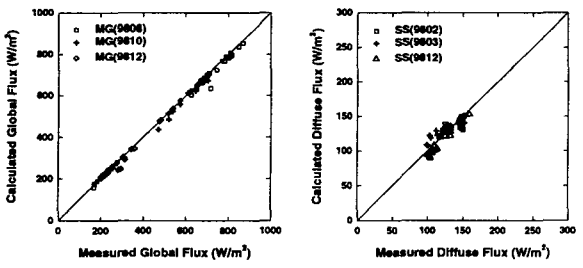

Fig. 2 (a): Scatterplots of downward surface solar flux between the simulated and measured global flux at Mandalgovi (left) and diffuse flux at Sri-Samrong (right) under the clear sky condition.

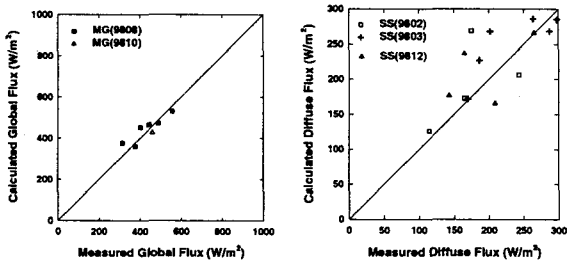

Fig. 2 (b): Same as in Fig. 2 (a) except the cloudy sky condition.

3.3 Aerosol radiative forcing

Aerosol radiative forcing was calculated using the measured aerosol optical properties derived from sky radiation measurements in conjunction with a radiative transfer model. In order to avoid the dependence on solar zenith angle in aerosol radiative forcing calculation, we use 24-hour averaged radiative forcing. In the calculations, constant aerosol optical thickness is assumed throughout the day.

Fig. 3 (a) shows efficiency of 24-hour mean aerosol radiative forcing (Wm^{-2}) $\Delta F/\Delta\tau_{0.7}$ evaluated from the aerosol optical parameters. The aerosol single scattering albedo ($\omega_{0.7}$) and 1st and 2nd moments, g_1 and g_2 of the aerosol phase function are also shown in Fig. 3 (b). The results show that downward fluxes are varied with aerosol changes in the range of -100 to -170 W m^{-2} per unit $\tau_{0.7}$ at the surface. The difference among the stations is deeply related to the differences in single scattering albedo ($\omega_{0.7}$) and asymmetric parameter (g_1). The surface aerosol forcing at Amami-Oshima and Mandalgovi shows very small values, as $\omega_{0.7}$ and g_1 are smaller than other stations. Since these lower values of single scattering albedo than other sites would be reflected to magnitude of aerosol radiative forcing, which might be larger radiative forcing at surface owing to increases of atmospheric absorption over East Asian region.

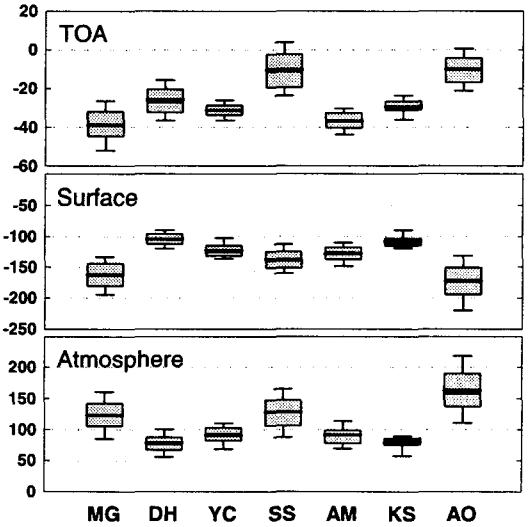

Fig. 3 (a): Range of 24-hour average aerosol radiative forcing (Wm^{-2}) per unit aerosol optical thickness at 0.7 μm. Each line in box plots means that median, and 10th,

25th, 75th, and 90th percentiles.

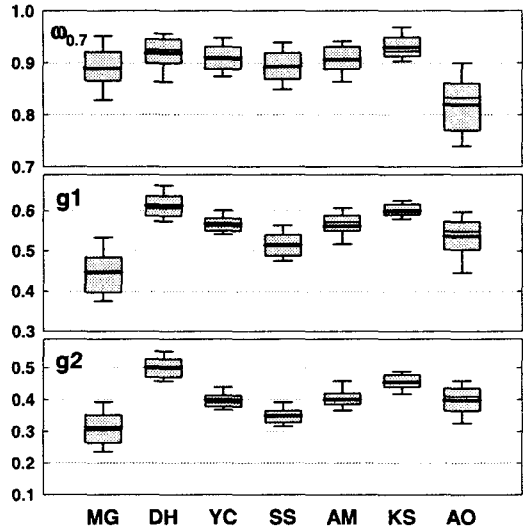

Fig. 3 (b): Same as in Fig. 3 (a) except basic aerosol optical parameters.

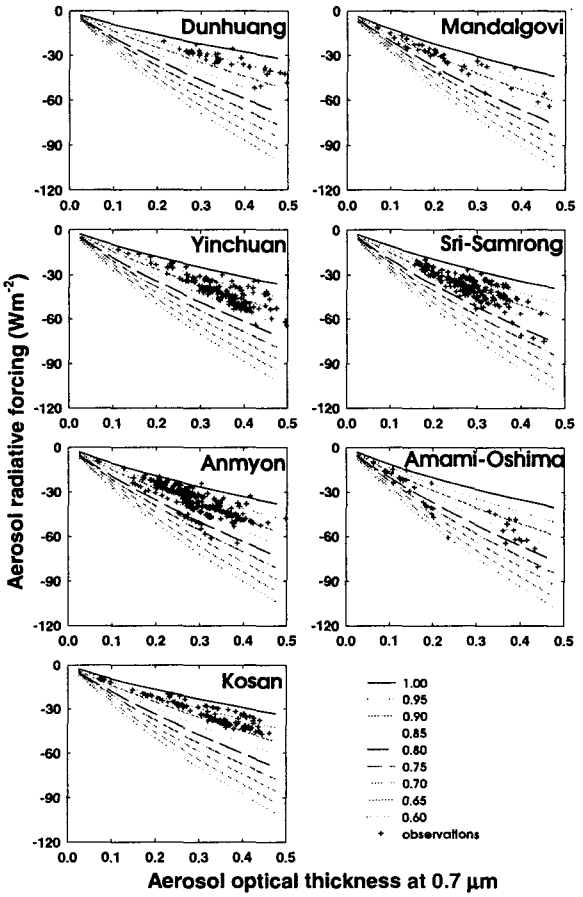

Fig. 4: 24-hour averaged aerosol radiative forcing with aerosol optical thickness at the wavelength of 0.7 μm. Theoretical lines are various values of single scattering albedo at 0.7 μm.

Fig. 4 shows the 24-hour mean clear sky radiative forcing for the corresponding aerosol parameters as a function of aerosol optical thickness at 0.7 μm with various values of single scattering albedo. We used the averaged values of g_1 and g_2 at each site. It is found that the optimal single scattering albedo value has a characteristic dependence on atmospheric turbidity and different geographic locations.

Optical properties ($\omega_{0.7}$, g_1 and g_2) and related radiative forcing at Amami-Oshima are found to be much different from those two close sites (Kosan, Anmyon), suggesting there are different aerosol processes around Amami-Oshima. Under the westerlies, Korean and Japanese atmosphere are much affected by the gases and aerosols originated from Chinese area. As aerosol optical characteristics are important to radiative forcing both at surface and the TOA, the mixing process as well as the emission from various sources would alter the magnitude of aerosol forcing by changing the optical and chemical properties during the movement of aerosols.

4. Conclusions

Aerosol optical characteristics of East Asia are complicated mixture of various aerosols: such as, absorbing soot, organic aerosols by coal and biomass burning, and Asian dust. Thus, aerosol radiative forcings both at the surface and the TOA show wide variations depending on geographical locations, due to the prevalent aerosol types. Ranges were from -100 to -170 Wm^{-2} for the surface and -10 to -40 Wm^{-2} for the TOA.

5. Acknowledgments

This research has been supported by the CES funded through KOSEF.

6. References

Charlson, R. J., S. E. Schwartz, J. M. Hales, R. D. Cess, J. A. Coakley Jr., J. E. Hansen, and D. J. Hofmann, 1992: Climate forcing by anthropogenic aerosols. *Science*, 255, 423-430.

Eck, T.F., B.N.Holben, J.S.Reid, O.Dubovik, A.Smirnov, N.T.O'Neill, I.Slutsker, and S.Kinne, 1999: Wavelength dependence of the optical depth of biomass burning, urban and desert dust aerosols, *J. Geophys. Res.*, 104, 31 333-31 350.

Eck, T.F., B.N. Holben, D.E. Ward, O. Dubovik, J.S. Reid, A. Smirnov, M.M. Mukelabai, N.C. Hsu, N.T. O'Neill, and I. Slutsker, 2001: Characterization of the optical properties of biomass burning aerosols in Zambia during the 1997 ZIBBEE field campaign, *J. Geophys. Res.*, 106, 3425-3448.

Hansen, J., M. Sato, A. Lacis, and V. Oinas, 2000: Global warming in the twenty-first century: An alternative scenario. *Proc. Natl. Acad. Sci.* USA, 97, 9875-9880.

Haywood, J. M., and V. Ramaswamy, 1998: Global sensitivity studies of the direct radiative forcing due to anthropogenic sulfate and black carbon aerosols. *J. Geophys. Res.*, 103, 6043-6058.

IPCC, 2001, Climate change 2001: Scientific Basis. Contribution of Working Group I to the Third

Assessment Report of the Intergovernmental Panel on Climate Change [Houghton, J.T., L.G. Meira Filho, B.A. Callander, N. Harris, A. Kattenberg, and K. Maskell (eds.)]. Cambridge University Press, Cambridge, United Kingdom and New York, NY, USA, 881 pp.

Jacobson, M. Z., 2001: Strong radiative heating due to the mixing state of black carbon in atmospheric aerosols, *Nature*, 409, 695-697.

Kaufman, Y. J., A. Gitelson, A. Karnieli, E. Ganor, R. S. Fraser, T. Nakajima, S. Mattoo, and B. N. Holben, 1994: *J. Geophys. Res.*, 99, 10341-10356.

Lohmann, U., J. Feichter, J.E. Penner, and R. Leaitch, 2000: Indirect effect of sulphate and carbonaceous aerosols: A mechanistic treatment, *J. Geophys. Res.*, 105. 12,193-12,206.

Markham, B.L., J.S. Schafer, B.N. Holben, and R.N. Halthore, 1997: Atmospheric aerosol and water vapor characteristics over north central Canada during BOREAS, *J. Geophys. Res.*, 102, 29737-29745.

Nakajima, T and T. Nakajima, 1995: Wide-area determination of cloud microphysical properties from NOAA AVHRR measurements for FIRE and ASTEX regions. *J.A.S.*, 52, 4043-4059.

Nakajima, T and M. Tanaka, 1988: Algorithms for radiative intensity calculations in moderately thick atmospheres using a truncation approximation, *J. Quant. Spectrosc. Radiat. Transfer*, 40, 51-69.

Nakajima, T., G. Tonna, R. Rao, R. Boi, Y. Kaufman, and B. Holben, 1996b: Use of sky brightness measurements from ground for remote sensing of particulate polydispersions, *Applied Optics*, 35, 2672-2686.

Nakajima, T. and A. Higurashi, 1997: AVHRR remote sensing of aerosol optical properties in the Persian Gulf region, summer 1991. *J. Geophys. Res.*, 102, 16935-16946.

Okada, I., T. Takamura, K. Kawamoto, T. Inoue, Y. Takayabu, and T. Kikuchi, 2000: Cloud cover and optical thickness from GMS-5 image data. *Proc. GAME AAN/Radiation Workshop*, Phuket, 8-10 March, 2001, 9-11.

Russell, P. B., J. M. Livingston, P. Hignett, S. Kinne, J. Wong, A. Chien, R. Bergstrom, O. Durkee, and P. V. Hobbs, 1999: Aerosol-induced radiative flux changes off the United States mid-Atlantic coast: Comparison of values calculated from sunphometer and in situ data with those measured by airborne Pyranometer. *J. Geophs. Res.* 104, 2289-2307.

Satheesh. S. K., V. Ramanathan, Xu Li-Jones, J. M. Lobert, I. A. Podgorny, J. M. Prospero, B. N. Holben, and N. G. Loeb, 1999: A model for the natural and anthropogenic aerosols over the tropical Indian Ocean derived from Indian Ocean Experiment data. *J. Geophys. Res.*, 104, 27421-27440.

Schwartz, S. E., 1996: The whitehouse effect – shortwave radiative forcing of climate by anthropogenic aerosols: An overview. *J. Aerosol Sci.*, 27, 359-382.

Shine, K.P. and P.M. de F. Forster, 1999: The effects of human activity on radiative forcing of climate change: a review of recent developments. *Global and Planetary Change*, 20, 205-225.